Volume 16, Number 4, 2023. pp. 447-455

Jordan Journal of Physics

ARTICLE

10 Hz Stable Mode-locked Er-Fiber Laser

F. Qamar

Physics Department, Faculty of Sciences, Damascus University, Damascus, Syria.

Doi: https://doi.org/10.47011/16.4.7

Received on: 22/11/2021; *Accepted on: 21/03/2022*

Abstract: In this paper, a stable output at the reduction repetition rate from 80 MHz mode-locked Er-doped fiber laser (EDFL) was demonstrated by adjusting the operating point for external $LiNbO_3$ Mach-Zehnder electro-optic intensity modulator to suppress harmonic mode-locked pulses. More than 70% of the laser beam was launched into the external pigtail Mach-Zehnder intensity modulator using single mode fiber with collimating lens and fiber (ferrule connector) FC adapter. The optimum values of Mach-Zehnder modulator bias voltages V_0 and V_π (half wave voltage) which resulted in maximum and minimum laser output power to leave the modulator were found at 6.5 and 0.29 V, respectively. The best modulation was achieved for the RF modulating signal with an opening time of about 8 ns. For driving voltage equal to V_π, a clean mode-locked pulse train was generated with a pulse shape and energy similar to the input pulse, albeit with a low repetition rate. The minimum repetition rate reached as low as 10 Hz, resulting in pulse energy and peak power of 0.32 nJ and 1.5 kW, respectively. Second-harmonic generation of the low repetition rate pulse train was also produced by using a PPLN crystal. This opens up the potential for using this laser in single photon detection experiments and as a seed laser for many applications.

Keywords: Er-fiber laser, Passively mode-locked fiber laser, Nonlinear polarization rotation, Mach-Zehnder modulator, Fast electro-optic modulator.

PACS: Fiber lasers, 42.55.Wd, Mode locking, 42.60.Fc.

1. Introduction

Ultra short pulse fiber lasers represent compact, low-maintenance, and alignment-free light sources with superior thermal handling capabilities, making them suitable for a wide range of applications. Typically, generating ultra-short pulses in fiber laser relies on the contribution of fiber nonlinearity, which could induce instability or even collapse of the pulse [1]. Moreover, in passively mode-locked lasers, the presence of fiber nonlinearity limits the repetition rate of fs-pulses. This limitation arises from the strong nonlinearity in the cavity, which necessitates high pulse energy [2, 3], while the repetition rate is fixed by cavity length. On the other hand, the repetition rates of fs pulse trains in actively mode-locked fiber lasers tend to be larger. This is because the pulse train in these lasers is based on soliton pulse shaping, which requires a longer cavity to accumulate sufficient nonlinearity. However, this extended cavity length increases the cavity instability [4, 5]. Nevertheless, there have been instances where mode-locked fiber lasers operated at low repetition rates (~ 191 kHz) within a linear cavity, facilitated by using a high modulation depth semiconductor saturable absorber mirror (SESAM) [6]. In contrast, the only way to obtain ultra-low repetition rate fs pulse train out of fiber ring cavity laser systems is to suppress pulses using external modulators. Femtosecond source

Corresponding Author: Fadi Qamar **Email**: fadiqamar@Hotmail.com

systems with low repetition rates, ranging from a few hundred hertz have found applications in various fields, including nuclear and radioactivity research [7], free electron laser (FEL) and single photon studies [8], electronics manufacturing (for tasks such as writing waveguides [9]), and industrial applications like direct welding of glass and metal [10]. Integrated intensity Mach-Zehnder modulator (MZM) represents a powerful means for externally modulating the optical signal and can also be used for suppressing a steady harmonic mode-locked pulse. An MZM device is described as a two-waveguide-arms interferometer integrated in either silicon [11, 12] or in $LiNbO_3$ substrates [13]. The waveguides are linked together through the input (E_{in}) and output (E_{out}) optical Y junctions. Adjacent to the waveguides, a system of electrodes is strategically placed to generate an electric field effectively within the waveguide region. Commercially available modulators are usually equipped with separate radiofrequency (RF) and bias ports, as shown in Fig. 1.

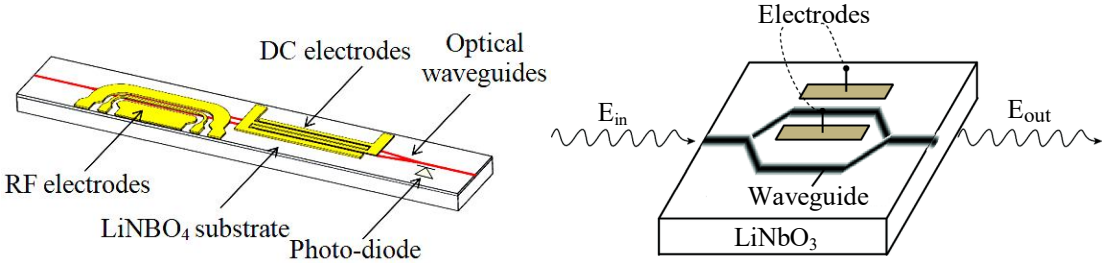

FIG. 1. Configuration and schematics of integrated intensity MZM.

The RF port provides a balanced 50 Ω input for broadband modulating signal. The input driving voltage for the desired operating point set-up is supplied by the bias port. The applied voltage to the electrical input (either the bias one or the modulating one) modifies the refractive index of the $LiNbO_3$ substrate.

This causes a phase shift between the light waves moving through the particular waveguides. A zero phase shift between the waves yields constructive recombination, leading to the maximum intensity at the output pigtail. Conversely, a π phase shift (opposition shift) produces destructive recombination, resulting in minimal radiation leaving the modulator's output pigtail. A gradual transition between these two extremes allows for a smooth change of output optical power. Considering the excitation of only one electrical port of the MZM at the time (the bias port for instance), the idealized transfer chart can be described by cosine function [14]:

$$P_0 = \frac{P_{in}\alpha}{2}\left[1 + cos\left(\frac{V_{in}}{V_\pi}\pi\right)\right]$$

where P_o and P_{in} are output and input optical powers, respectively, V_{in} is the input voltage of the bias port, V_π is the half-wave voltage of the bias port, and α is the insertion loss of the modulator. Some manufacturers equip their modulators with an auxiliary - in substrate buried photodiode (PD). The PD is located just behind the output Y junction. An advantageous aspect of this configuration is that the PD signal can be used to monitor the modulator's output, eliminating the need for an external tap-coupler. A comprehensive model-based bias controller has been introduced for a Mach-Zehnder intensity modulator, aimed at regulating the bias voltage to uphold the operating point deviation of the modulator. This approach relies on directly computing the operating point deviation through an analysis based on a fast Fourier transform, with an accurately set level of vector averaging [15]. Utilizing MZM with EDFLs has been reported in different publications as an intracavity element that is used to actively mode-lock the laser [16], suppress the intracavity noise [17], and create a stabilized multi-wavelength laser ring cavity [18, 19].

This paper introduces a novel application of an intensity MZM with EDFL. To the best of my knowledge, this marks the first use of the MZM as an external cavity element, attached to a passively mode-locked Er-doped fiber laser ring cavity, to obtain a fs pulse train with a very low repetition rate (10 Hz). The parameters of intensity MZM for the stable operation were experimentally discovered and the jittering time of the pulse was minimized using feedback triggering. SHG for the low repetition rate output of the mode-locked (ML) fiber laser was also demonstrated.

2. Experimental setup

The experimental arrangement is schematically shown in Fig. 2.

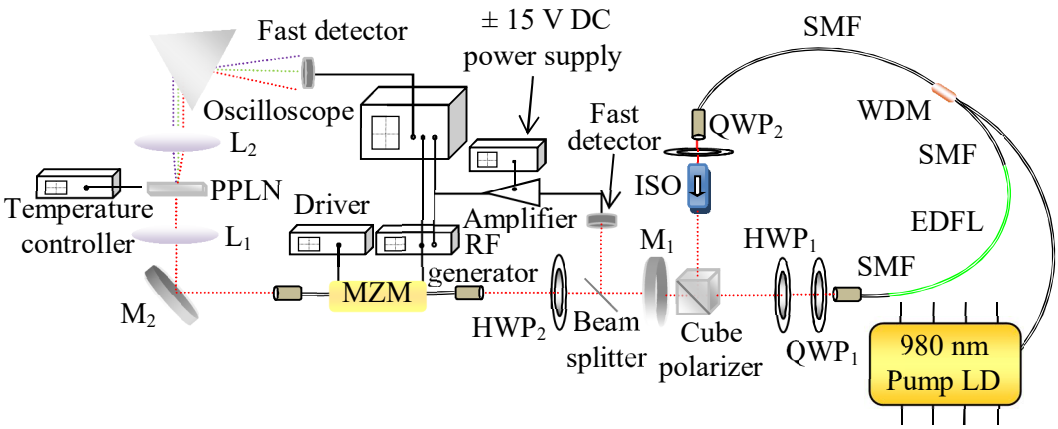

FIG. 2. Experimental arrangement for pulses suppression of ML Er-fiber laser using Mach-Zehnder electro-optic modulator.

The laser cavity consists of 40 cm EDFL (80-8/125 from Thorlabs), 230 cm single-mode fiber (SMF) at 1550 nm, and 30 cm free space section. The free space section is configured in an L-shape and includes a cube polarizer that functions as the output coupler and is positioned at the corner. The first arm of the free space section is 12 cm long and includes a quarter-wave plate (QWP_1) and a half-wave plate (HWP_1), while the second arm is 18 cm long and includes a QWP_2 followed by an isolator (ISO). All polarization elements operate at 1550 nm. Single mode EDFL is pumped by semiconductor diode laser (Bookham - LC96UD74 - 2DR) through wave division multiplexing (WDM). The center wavelength of the pumping diode is 974 nm measured at 15 °C and is controlled by Newport laser diode controller model 6000. The laser was mode-locked via nonlinear polarization rotation (NPR) by polarization elements. The ML output beam is then passed from the polarized cube to the mirror labeled as M1. M1 is a high reflection (HR) mirror designed to reflect light at 980 nm and transmit light at 1.5 μm, serving to filter out the pumping wavelength, which is 980 nm. Since MZM is polarization sensitive, a half-wave plate HWP_2 is used to rotate the ML beam polarization to achieve a maximum output from MZM. The MZM (Mach-10™ 056 from COVEGA) is an intensity modulator with an integrated photo-detector and is designed to give a small form-factor modulation with an increase in bandwidth for forward error correction (FEC) implementation; supporting data rates from 9.953 Gb/s to 12.5 Gb/s. The Intensity MZM is based on Titanium-in diffused x-cut lithium niobate and uses a Mach-Zehnder interferometric architecture. The light beam launched into MZM via a collimation lens. The MZM was driven by the Photline MBC-1001 modulator bias controller to provide bias voltage V_π. Radio frequency (RF) for MZM was provided by a digital delay frequency generator (P400 DDG) from Highland Technology. A fast InGaAs detector (Et 3500 from E. O. Tech.) and a single amplifier are used to detect and amplify a small part of the ML signal that was excreted by the beam splitter before MZM. The ML signal can be used to trigger the RF generator. Another similar fast detector was also used to monitor the signal after MZM. The RF generator and the two fast detectors are connected to four-channel wave runner 44 xi 400 MHz, 5 Gs/s oscilloscope from Teledyne Le Croy Corporation. This allows to monitor MZM input and output signals as well as RF modulation signals at the same time. The output beam MZM can also be launched by a collimator to a 90:10 fiber beam splitter that directs the large part of the beam to a Thorlabs power meter to measure its power, while a smaller portion of the beam is routed to an AQ6315E optical spectrum analyzer (ranged from 350 to1700 nm) to measure the wavelength. However, the second harmonic generation (SHG) of the modulated signal can be generated by the PPLN nonlinear crystal. For this, 45°the HR at 1560 nm M_2 dielectric mirror was inserted into the beam bath after MZM to reflect the fundamental beam into PPLN crystal. The crystal was positioned between two con-

focal coated lenses, denoted as L_1 and L_2. It was mounted on a temperature-controlled oven to optimize the quasi-phase matching (QPM) condition for each harmonic wavelength. Both lenses had the same focal lengths of 15 mm, and they were configured in such a way that the beam focused to approximately a 50 μm spot radius in the center of the crystal. This satisfied the optimum con-focal condition for PPLN crystal. The lenses had different coatings: L_1 had an HT coating at the fundamental beam wavelength of 1550 nm, while L_2 was coated with HT at the SHG beam wavelength of 800 nm. A Si fast detector from E. O. Tech. was also used to measure the pulse trains for the harmonic generations after they were separated by a suitably coated prism and blocking the fundamental light by using a band-pass filter placed after the L_4 lens.

3. Results and Discussion

Before operating MZM, a clean train of ML pulses with an average power, pulse period, and repetition rate of 72 mW, 12.4 ns (cavity single trip), and 80.6 Hz, respectively, was obtained from EDFL via NPR. The wavelength spectrum showed that the lasing wavelength was centered at about 1558 nm with an FHWM of 13.68 nm. The duration of the single pulse of the ML pulse train was calculated using previous values and found to be about 184 fs. The ML pulse train was launched through a collimated lens to SMF at 1550 nm and connected to the pigtail fiber of the MZM via a PC fiber connector. This allowed only 53 mW to be launched into MZM. The DC bias voltage of MZM was then varied to observe the maximum and minimum output power of the transmitted beam. The minimum output power (nearly zero) was obtained at the voltage V_π of 0.29 V while the maximum output power of 26.3 mW was achieved when V_0 of 6.5 V (Fig. 3). However, one of the major problems linked with the practical application of Mach-Zehnder intensity modulators is drifting the operating point. The drift is caused by pyroelectric, photorefractive, and photoconductive phenomena that take action simultaneously in the $LiNbO_3$ substrate [10]. This explains why the maximum value of the output has not been found at zero voltage in Fig. 3.

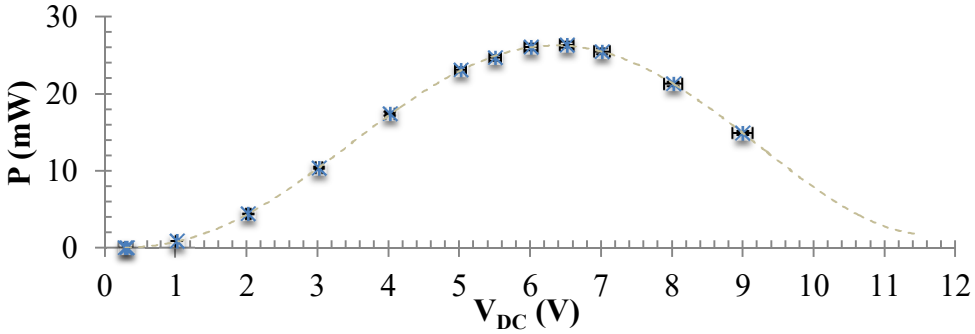

FIG. 3. Bias voltage V_{DC} versus the MZM output power. V_0 and V_π were found at 6.5 V and 0.29 V.

The time profiles of MZM input and maximum output pulse trains (Fig. 4) confirm that there is no change in repetition rate between the two pulse trains when no RF modulation signal was applied. However, the time shift between the two signals was due to the refractive indices difference of optical paths through which the signals propagate.

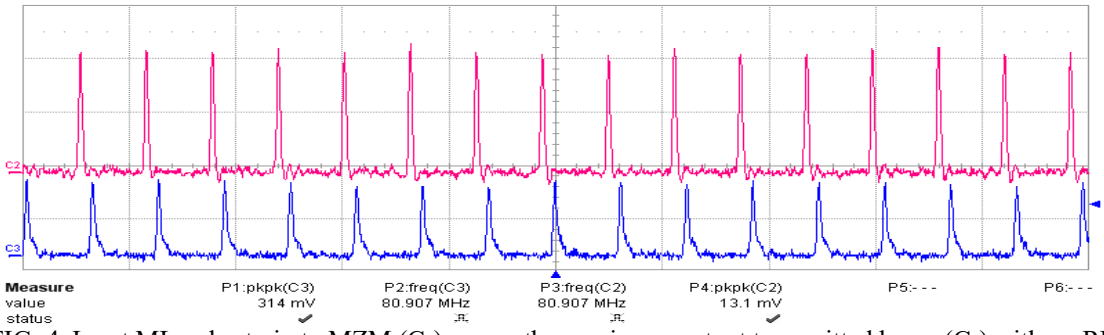

FIG. 4. Input ML pulse train to MZM (C_2) versus the maximum output transmitted beam (C_3) with no RF modulation signal being applied.

Applying the RF modulation signal on the MZM, which operated at V_0 = 6.5 V, led to the suppression of certain pulses from the input ML pulse train (Fig. 5). The pulse duration and the repetition rate of the RF signal were 139.4 ns and 5.05 MHz, respectively. These resulted in a duty cycle of 70.45%. As a consequence, the maximum output power decreased to 16.4 mW.

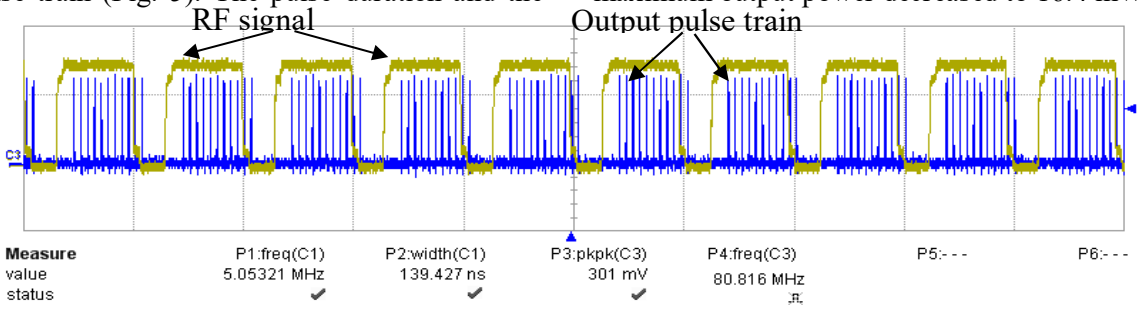

Fig. 5. Output modulated signal of MZM operated at 6.5 V when 5 MHz RF signal with an opening window of 139.4 ns is applied.

Further adjustments to the opening time and the repetition rate of the modulated RF signal led to the suppression of only one pulse of the ML pulse train, as shown in Fig. 6. This was done when the pulse duration from the RF generator was at 8.4 ns, utilizing the maximum modulation frequency available value (10.1 MHz). The duty cycle of the pulse generator was 8.5% resulting in an output ML pulse train from MZM with an average power of 21.2 mW.

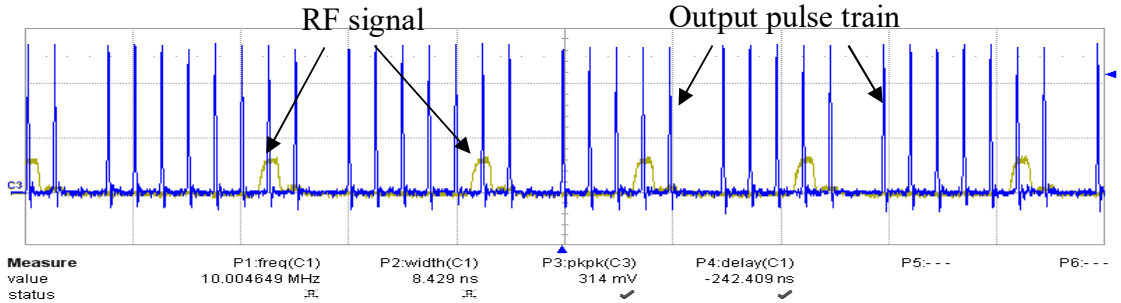

FIG. 6. Output modulated signal of MZM operated at 6.5 V when a10 MHz RF signal with an opening window of 8.4 ns was applied.

The previously suppressed pulse reappeared, while other pulses began to disappear when the DC bias voltage decreased. Figure 7 shows the case when the DC bias is decreased to approximately half of its original value (i.e. 3.22 V). This reduction caused the MZM output power to decrease to 9.6 mW.

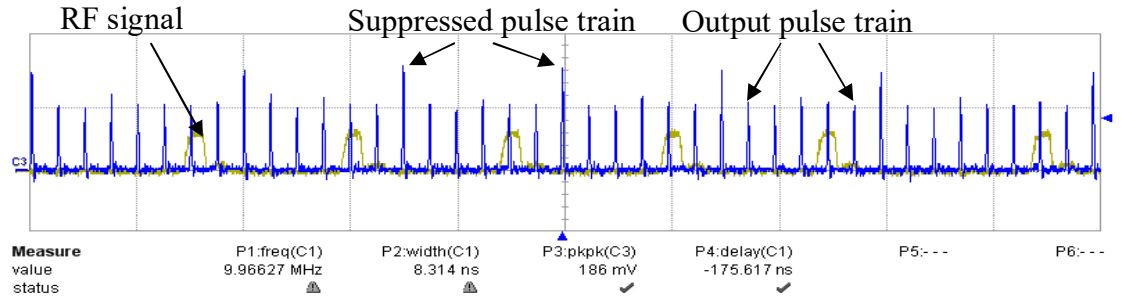

FIG. 7. The output modulated signal of MZM when operated at DC voltage 3.22 V and when a 10 MHz RF signal with an opening window of 8.4 ns is applied.

All intra-ML pulses completely disappeared (as shown in Fig. 8) when the bias voltage was reduced to its minimum value of 0.29 V, despite using the same modulation signal frequency (10.1 MHz) and pulse width (8.4 ns). The average output power in this case was 3.2 mW.

Figure 9 shows the comparison between the input pulse train with a repetition rate of 80.7 MHz and the output pulse train with a pulse repetition rate of 10.1 MHz.

However, decreasing the opening time of the RF square pulse under 8.4 ns affected the pulse stability, as shown in Fig. 10.

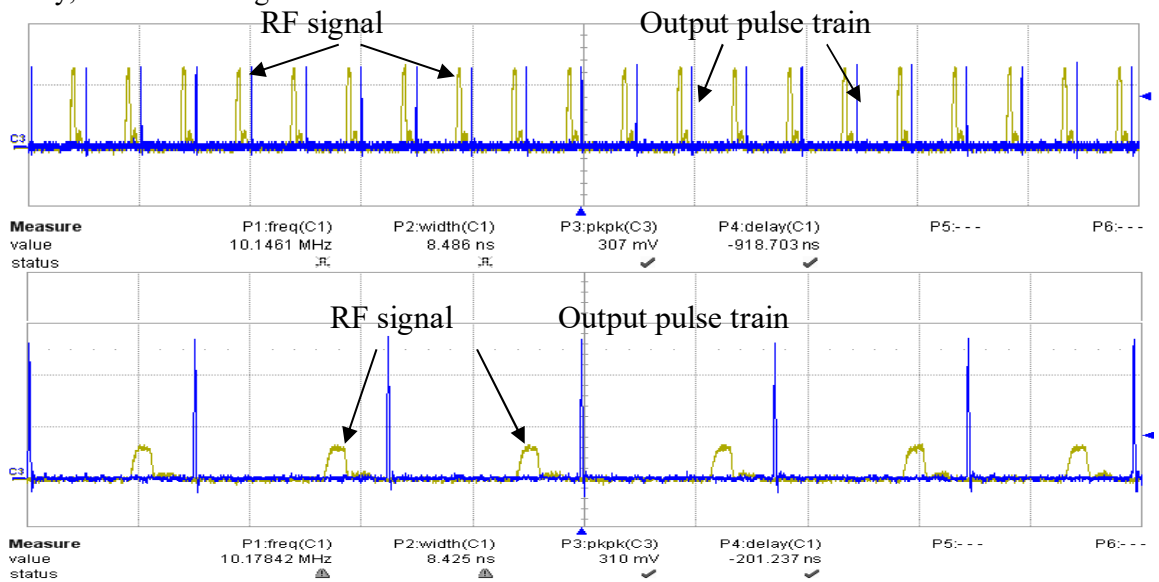

FIG. 8. The modulated signal output (at different time scales), when MZM operated at half wave DC voltage V_π = 0.29 V and RF signal with a frequency of 10 MHz and an opening window of 8.4 ns.

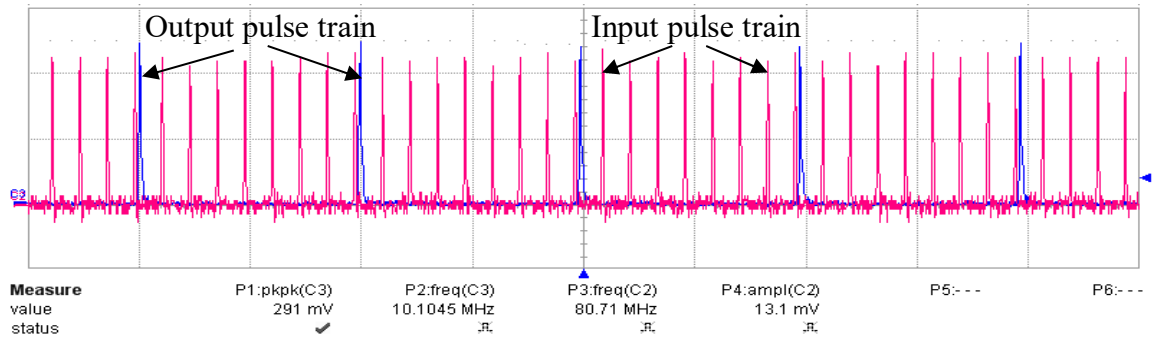

FIG. 9. The comparison between the MZM input pulse train and the output modulated signal, when MZM operated at 0.29 V (half-wave voltage) with an RF frequency of 10 MHz and an opening window of 8.4 ns being applied.

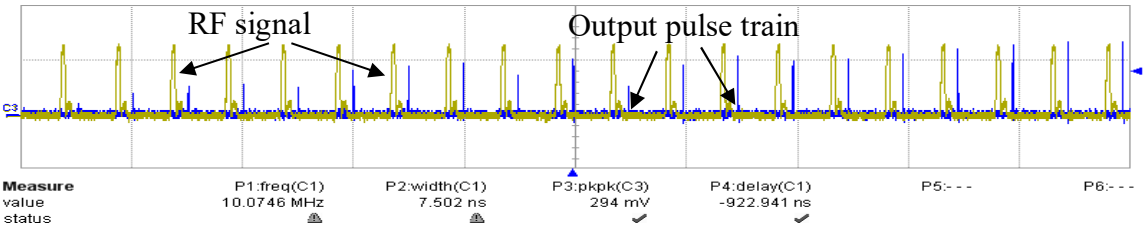

FIG. 10. Instable output pulse train signal when the opening time of the RF modulating signal is reduced below 8.4 ns.

On the contrary, the frequency modulation of the pulse can be reduced to nearly 10 Hz without affecting the stability of the ML train pulse or reducing pulse amplitude (Fig. 11). The average power output of the 10 Hz pulse train was about 3.2 nW. This resulted in an energy per pulse and pulse peak power of 0.32 nJ and 1.5 kW, respectively. Reducing the frequency modulation below 10 Hz also affected the pulse stability and made it difficult to generate a steady signal.

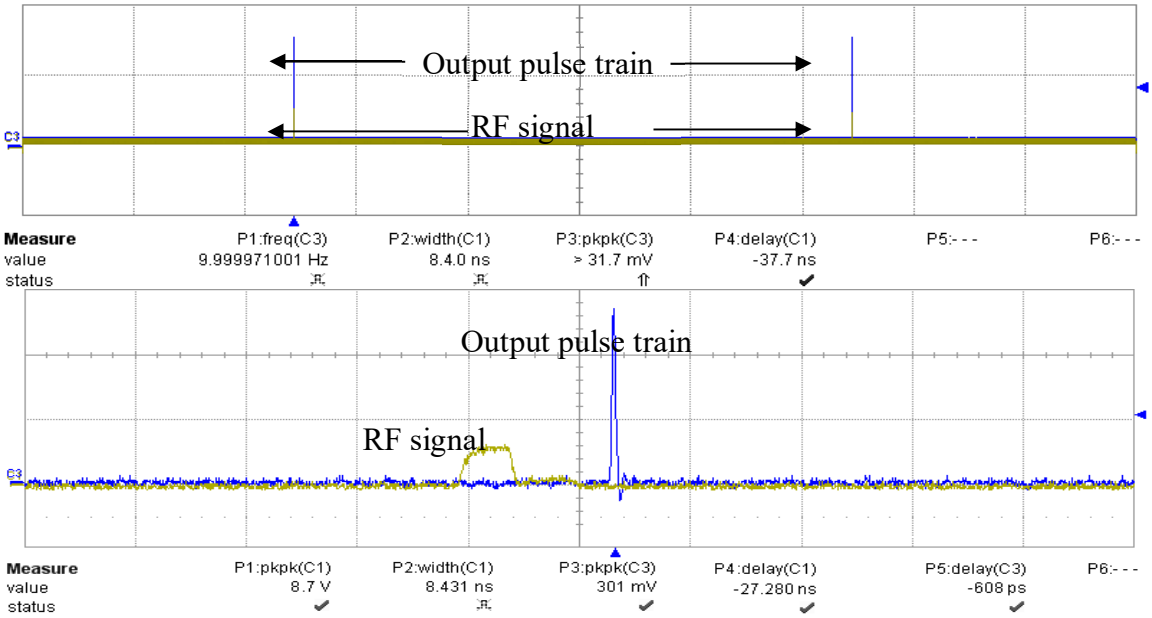

FIG. 11. 10 Hz stable modulated signal output at different time scales.

The average output power of the modulated pulses was measured as a function of the RF signal frequency, which is equal to the repetition rate of pulse train. The resulting curve confirmed a linear relationship (Fig. 12) where $P_{av} = E_p * f$.

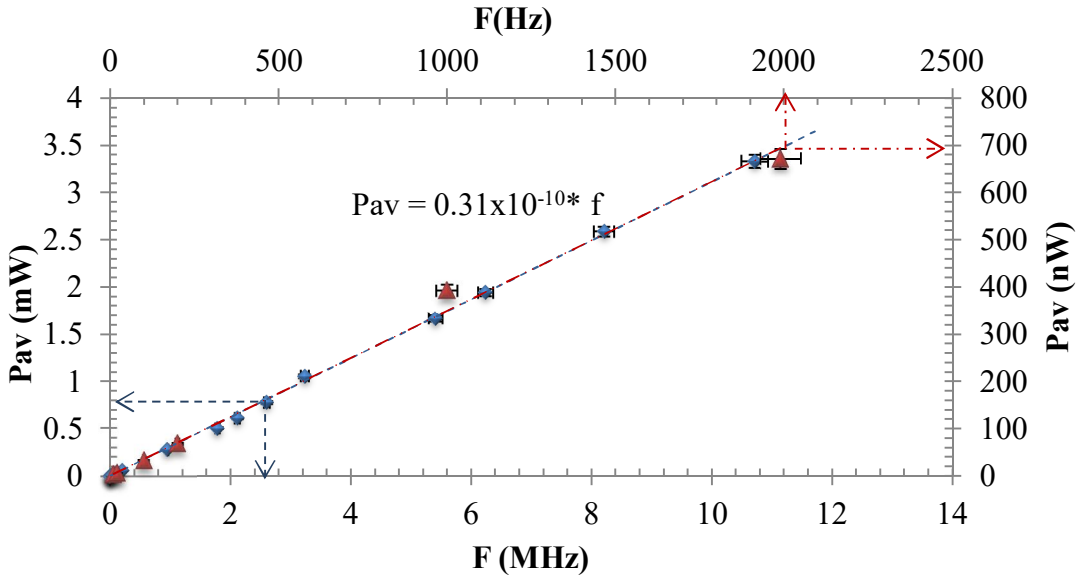

FIG. 12. The average power output as a function to modify the RF signal frequency.

To overcome the huge time jittering of RF and increase the stability of the modulated pulse train, it was necessary to trigger the RF generator by a segment from the original ML beam (i.e. triggering with a feedback signal). This can be done by using a beam splitter after the mirror M_1, a fast detector to detect the segment optical signal, and an operational amplifier to amplify the detected signal before triggering the RF generator (Fig. 2). After triggering by a feedback signal, the time jittering for the RF signal reduced from 5 ns to 0.36 ns and for the ML pulses from 373 ps to 28.6 ps.

The effect of MZM on ML pulse width was also investigated by comparing the FWHM of the wavelength spectrum of the beam before the MZM with the FWHM after modulation, as illustrated in Fig. 13. The width of the input signal spectrum reduced from 13.68 nm to 12.06 nm when the signal passed through the MZM. Thus, the MZM leads to an increase in the width of the input ML pulses. Calculations showed that the pulse width increased from 184 fs to 212 fs (i.e. more than 13%), indicating the need for a compression process to reduce the pulse width again.

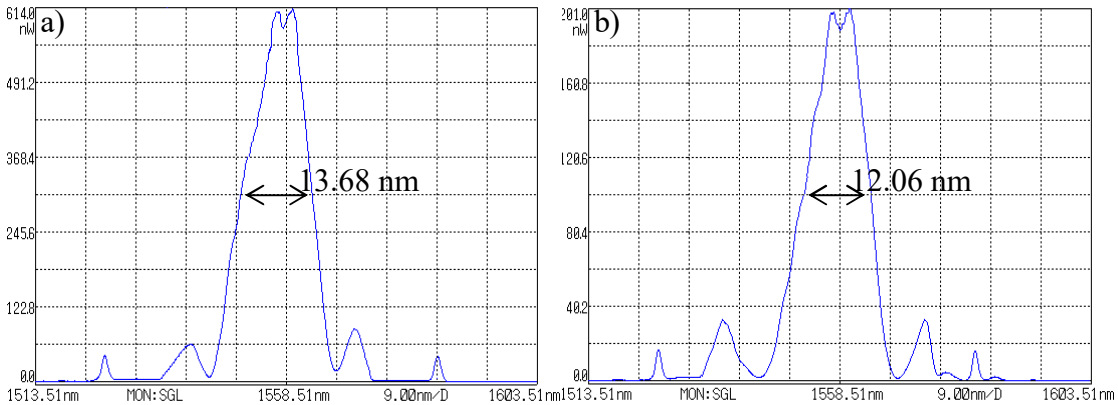

FIG. 13. a) Spectrum of the input signal, b) Spectrum of MZM output signal.

SHG of 10 Hz ML pulse train (Fig. 14) was also generated using a PPLN crystal operated at 34°C. The energy of a single SHG pulse was estimated to be 0.03 nJ with a pulse duration of 162 fs centered at a wavelength of 779 nm.

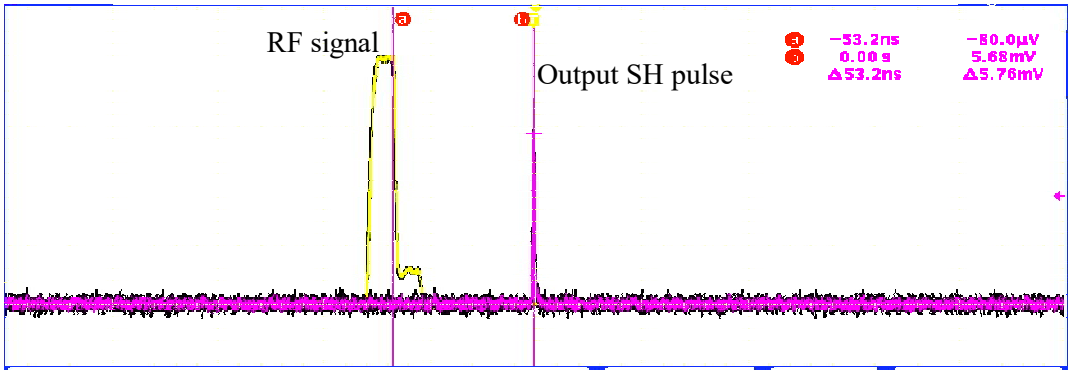

FIG. 14. SHG signal for 10 Hz ML plus train.

4. Conclusion

The ultra-low repetition rate of the femtosecond pulse train was successfully accomplished using ML EDFL with external MZM. The EDFL was ML via NPR using three wave plates. The ML pulse train had a repetition rate of about 80 MHz and an average power of 73 mW. However, only 52 mW of this power was launched to MZM due to the launching and fiber connector losses. The maximum output of 26.3 mW from MZM with no modulation was obtained for bias DC voltage V_0 = 6.5 V while the minimum value was observed at V_π = 0.29 V. To suppress the pulses, the MZM was operated at the V_π while the RF signal was applied. A stable fs pulse train with an average power of 3.2 nW and a repetition rate of 10 Hz was achieved. Time jittering of the RF and the modulated signal was reduced to 0.36 ns and 28.6 ps, respectively, when the RF generator was triggered by feedback from ML's original signal. Effects of modulation on the pulse of the ML beam were also investigated and results showed that the modulator enlarged the pulse width more than 13% of its original one. SHG with a low-frequency ML pulse train centered at 779 nm was achieved as well using PPLN crystal. However, the pulse energy of the low-frequency ML can be amplified by conventional methods, making it suitable for a wide range of applications.

References

[1] Anderson, D., Desaix, M., Lisak, M. and Quiroga-Teixeiro, M.L., J. Opt. Soc. Am. B, 9 (8) (1992) 1358.

[2] Chong, A., Buckley, J., Renninger, W. and Wise, F., Opt. Exp., 14 (21) (2006) 10095.

[3] Haus, H.A., Tamura, K., Nelson, L.E. and Ippen, E.P., IEEE J. Quantum Electron., 31 (3) (1995) 591.

[4] Li, J., Andrekson, P.A. and Bakhshi, B., IEEE Photon. Tech. Lett., 12 (9) (2000) 1150.

[5] Nakazawa, M. and Yoshida, E., IEEE Photon. Tech. Lett., 12 (12) (2000) 1613.

[6] Zhang, M., Chen, L.L., Zhou, C., Cai, Y., Ren, L. and Zhang, Z.G., Las. Phys. Lett., 6 (9) (2009) 657.

[7] Fourmaux, S., Serbanescu, C., Kincaid, R.E., Krol, Jr.A. and Kieffer, J.C., Appl. Phys. B, 94 (4) (2008) 569.

[8] Baumler, W., Schmalzl, A.X., Gobi, G. and Penzkofer, A., Meas. Sci. Technol., 3 (1992) 384.

[9] Saliminia, A., Nguyen, N., Nadeau, M., Petit, S., Chin, S. and Vallée, R., J. Appl. Phys., 93 (2003) 3724.

[10] Green, W., Rooks, M., Sekaric, L. and Vlasov, Y., Opt. Exp., 15 (25) (2007) 17106.

[11] Zhang, G. and Cheng, G., Appl. Opt., 54 (30) (2015) 8957.

[12] Li, M., Wang, L., Li, X., Xiao, X. and Yu, Sh., Photonics Res., 6 (2) (2018) 109.

[13] Chen, A. and Murphy, E.J., "Broadband optical Modulators - Science, Technology and Applications", (CRC Press, 2012).

[14] Svarny, J., Proc. BEC, Tallinn, Estonia, (2010) 231.

[15] Svarny, J. and Chladek, S., J. Lightwave Technol., Early Access (2021).

[16] Wang, R., Dai, Y., Yin, F., Xu, K., Yan, L., Li, J. and Lin, J., Opt. Exp., 21 (18) (2013) 209.

[17] DePriest, C., Yilmaz, T., Delfyett, P., Etemad, S., Braun, A. and Abeles, J., Opt. Lett., 27 (9) (2002) 719.

[18] Pan, S. and Lou, C., IEEE Photon. Techn. Lett., 18 (13) (2006) 1451.

[19] Jain, A., Chandra, N., Anchal, A. and Kumar, P., Opt. & Las. Tech., 83 (2016) 189.